



## Case study

## Influence of a glass fiber mesh on pre-damaged flexible pavement's fatigue

Mateusz Kałuża<sup>1</sup>, Mirosław Kotasiński<sup>2</sup>, Joanna Bzówka<sup>3</sup>

**Abstract:** As part of a rehabilitation process, one lane of the pavement was reinforced with glass fiber mesh placed beneath the asphalt layer, while the other lane underwent rehabilitation without the mesh. To evaluate the performance of the pavement, the researchers used Falling Weight Deflectometer (FWD) measurements to assess the layer modulus, which is critical for understanding the structural capacity of the pavement. The fatigue life of the pavement was then calculated and compared against both the measured and predicted traffic load. The results indicated that the application of glass fiber mesh reinforcement positively impacted the pavement's structural integrity and durability. However, the beneficial effects were only observed after the mining activities that had initially caused damage to the pavement ceased. The pavement's fatigue life, based on dynamic load and traffic conditions, was compared between reinforced and unreinforced lanes, showing that the reinforced lane exhibited better resistance to damage once mining influences had concluded.

**Keywords:** Falling Weight Deflectometer, FWD equipment, flexible pavement, glass fiber mesh, mechanistic-empirical method, mining influence, pavement fatigue

<sup>1</sup>PhD., CEng., Certigos Engineering Sp. z o.o., ul. Brzezinska 8a, 44-203 Rybnik, Poland, e-mail: [mateusz.kaluza@certigos.pl](mailto:mateusz.kaluza@certigos.pl), ORCID: [0000-0002-9761-9066](https://orcid.org/0000-0002-9761-9066)

<sup>2</sup>PhD., Eng., Silesian University of Technology, Faculty of Civil Engineering, Akademicka 5, 44-100 Gliwice, Poland, e-mail: [miroslaw.kotasinski@polsl.pl](mailto:miroslaw.kotasinski@polsl.pl), ORCID: [0000-0002-5588-0741](https://orcid.org/0000-0002-5588-0741)

<sup>3</sup>Prof., DSc., PhD., CEng., Silesian University of Technology, Faculty of Civil Engineering, Akademicka 5, 44-100 Gliwice, Poland, e-mail: [Joanna.bzowka@polsl.pl](mailto:Joanna.bzowka@polsl.pl), ORCID: [0000-0002-1765-7354](https://orcid.org/0000-0002-1765-7354)

## 1. Introduction

Proper allocation of means between rehabilitation treatments and complete rebuilding of public road is an old dilemma among roads managements. Some of these problems require new and cost-effective solutions to prolong the fatigue resistance of a pavement construction, such as the application of geosynthetic layers under asphalt layers. Since rigid pavements are prone to their mining influences due to high rigidity modulus, flexible pavements are the only viable option. The influence of mining subsidence is hazardous to the durability and safety of pavement construction, leading to the problem of finding a proper solution to protect pavement construction from mining subsidence but also from typical damages, which applies to both new and rehabilitated roads [1, 2]. The road analyzed in this article lies in the mining subsidence area in Upper Silesia in Poland, where coal mining has led to ground deformation since the very beginning of the mining industry in the XIX century. The void in the rock massif after the coal excavation collapses over time and leads to the subsidence of the terrain [3]. The use of the geosynthetic layer as a subgrade reinforcement under mining influences in flexible pavement construction has been widely described [1–7]. The application directly on top of the old asphalt layer under the overlay allows delay or prevents crack propagation between layers [2, 4, 7]. The increase in pavement fatigue resistance was proven. The application below the subbase reduces the influence of horizontal unloading strain and is the most effective solution [1, 2]. Thus, it improves the resistance of the entire pavement construction to the loss of the equilibrium state from mining subsidence [1, 4, 7]. With the proper type of geosynthetic, the stiffness and bearing capacity of the asphalt layers is increased [6, 8, 9]. The correlations between selected deflection basin parameters and pavement moduli were previously studied; impact of applied reinforcement was proven [8, 9].

The analyzed road was rehabilitated in 2008 by milling the existing asphalt layers and applying new ones – 3-6 cm of leveling course 6 cm of binder course, and 4 cm of the surface course. During the process, one lane was reinforced with a glass fiber mesh applied to the existing construction under the base course, as shown in Fig. 1. The PGM-G50/50 glass fiber mesh has the following parameters:

- Tensile strength 50/50 kN/m,
- Tensile elongation of 3%,
- Tensile strength by elongation of 2% of 45 kN/m,
- Weight 350 g/m<sup>2</sup>,
- Recommended functions are separation, reinforcement, and stress dispersal.



Fig. 1. A glass fiber mesh located under the asphalt layers and an extracted asphalt core (Authors' photo)

The other lane was left without reinforcement. The existing structure consists of 20 cm of an aggregate base layer and 20 cm of crushed stone subgrade. The analyzed road was divided into 4 sections of 100 meters each; however, the last section was later abandoned due to traffic safety during the investigation. Each lane has a width of 3.0 m. The information obtained from the local mine indicates that it lies in the mining area of the total 1st category, and the measured subsidence from 2008 to 2019 was around 15 cm. In Fig. 2 the subsidence map is presented, together with the deformation parameters at 12 points of the analyzed road. The mining influences from the finished coal extraction of deposit 713 were present from 2008 to 2011 and from deposit 707 from 2016 to 2017. The presented parameters are:

- Inclination  $T$  [mm/m],
- Radius of curvature  $R$  [km],
- Horizontal strain  $\varepsilon$  [mm/m].

The research and analysis were conducted in 2016, eight years after rehabilitation treatments, and ended in 2023. The main purpose of the research led was to determine whether the glass fiber mesh reinforcement applied under asphalt layers was an effective solution for the pre-damaged flexible pavement impacted by mining influences. Changes in pavement life and bearing capacity were observed, determined and compared.

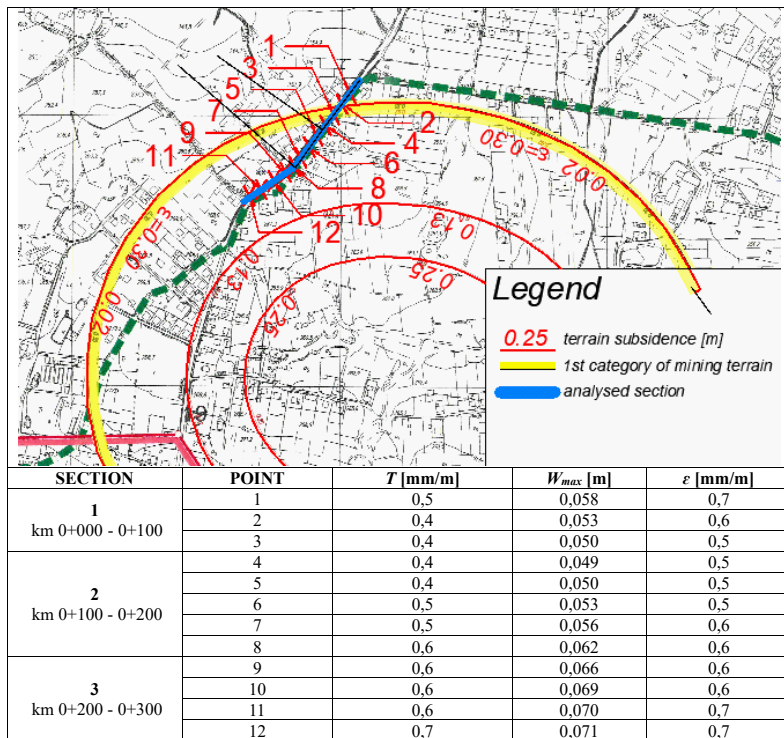


Fig. 2. Subsidence map with mining deformation parameters



Fig. 3. An example of analyzed section surface distresses (Authors' photos)

The cracking analysis was the first phase and the results indicated that the presence of the glass fiber reinforcement reduces the amount of crackings by 20% [7]. The next step was to investigate the influence of reinforcement on the parameters of the relationships between the deflection basin and the layers modulus and to analyze the developments of deflections and cracks between sections [7, 8]. The results showed that the applied reinforcement did not affect the values of the pavement deflection and the values of the deflection basin parameters. However, it affected the relationship between deflection basin parameters and the back calculated layer modulus; there was no relationship between the values in the reinforcement lane [9]. This may be caused by reinforcement that degrades the strength of the interlayer bond. In this paper, the influence of reinforcement on the fatigue life was investigated.

## 2. Materials and methods

Terrain research was conducted to identify vertical displacement, construction parameters, and pavement fatigue. A falling weight deflectometer was used and the measured data was supported by three 4.0 m drills to investigate the thickness of the subgrade and existing pavement layers. Pavement construction consists of the following layers:

- 1) Section 1 – km 0+000 to 0+100:
  - a) asphalt concrete – 12 cm,
  - b) crushed stone aggregate – 40 cm,
  - c) embankment (sand, crushed stone) – 60 cm.
- 2) Section 2 – km 0+100 to 0+200:
  - a) asphalt concrete – 17 cm,
  - b) crushed stone aggregate – 40 cm,
  - c) embankment (sand, crushed stone) – 60 cm.

3) Section 3 – km 0+200 to 0+300:

- a) asphalt concrete – 12 cm,
- b) crushed stone aggregate – 40 cm,
- c) embankment (sand, crushed stone) – 60 cm.

The subgrade consists of fine sands with clay sand in the medium dense state through stiff clay silt to silt sands with layers of fine silt in the medium dense state. For the backcalculation, the subgrade was unified. The  $\Delta E_{\text{sub}}$  range is from 43 to 70 MPa. The deflections were measured with a falling weight deflectometer (FWD) under a dynamic load of 50 kN. The geophones ( $D_1$ – $D_9$ ) were set at the following distances  $d_1 = 0.00$  m,  $d_2 = 0.20$  m,  $d_3 = 0.30$  m,  $d_4 = 0.60$  m,  $d_5 = 0.90$  m,  $d_6 = 1.20$  m,  $d_7 = 1.50$  m,  $d_8 = 1.80$  m,  $d_9 = 2.10$  m.

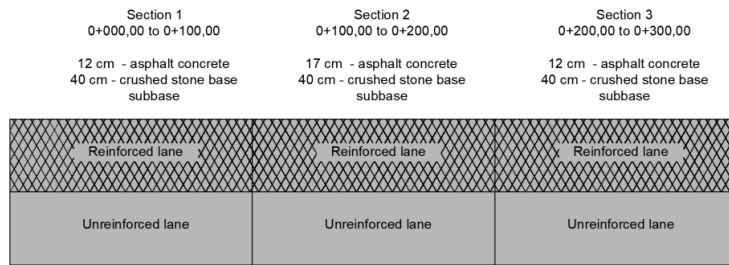


Fig. 4. Analyzed road’s section scheme

Measurements were taken in the mark of the right wheel every 25 m in each lane. The tests were carried out in August 2019 and September 2021. The data were used to backcalculate the modulus of the pavement layers and then to determine the strains at the bottom of the asphalt layer. These strains are crucial for the asphalt fatigue criterion to properly determine the remaining structural and functional life of the pavement. ELMOD software was used for backcalculation, using the best fit of the deflection basin between the measured and calculated theoretical deflection bowl. The different combinations of layer stiffness may produce the same bowl of deflection, and thus give improper values within the small range of error. This occurs more often in 4 and 5 layer pavement models and because of that similar layers were combined to create a 3 layer model. The modulus for asphalt concrete, subbase, and subgrade were calculated. The value of the deflection of the bowl is described with the following Eq. (2.1)

$$(2.1) \quad U_i = f(h, E, \nu)$$

where:  $U_i$  – deflection value at the  $i$ -point [ $\mu\text{m}$ ],  $f$  – functional dependence of component factors,  $h$  – thickness of each pavement layer [mm], [cm] or [m],  $E$  – modulus of the pavement layer [MPa],  $\nu$  – Poisson’s ratio [–].

Measured deflections were standardized to a load of 50 kN and a temperature of 20°C. The value of the Poisson ratio used for back calculation was  $\nu = 0.30$  for every layer. The modulus of the asphalt layers  $E_1$  were adjusted to a temperature of 20°C. To estimate the pavement fatigue of the analyzed road, the traffic load was measured for each lane to calculate the number of equivalent standard axis. The following periods were analyzed, from 2008 to 2019 and then

from 2019 to 2021. Traffic load is 8% higher in the reinforced lane than in the unreinforced one. The asphalt institute criterion was used, the strain at the bottom of the asphalt layer was calculated for the axle load of 100 kN for tire contact pressure of 700 kPa [7, 9]. The pavement scheme is presented in Fig. 5.

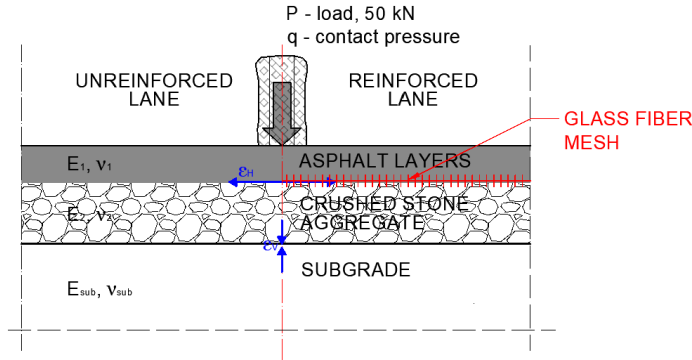


Fig. 5. Pavement's construction scheme

Bands software was used to estimate mixture parameters in 2008. The amount of binder was determined on extraction of the asphalt sample. The following parameters were used:

- 1) loading time of 0.02 s,
- 2) bitumen 35/50, bitumen stiffness modulus 34 MPa,
- 3) mixture density 2.68 Mg/m<sup>3</sup>,
- 4) apparent density 2,60 Mg/m<sup>3</sup>,
- 5) binder content of 5.5%,
- 6) voids content of 3.0%.

### 3. Results and conclusions

Asphalt layer modulus was calculated for asphalt 35/50 at a temperature of 20°C and resulted in a value of  $E_{2008} = 4360$  MPa. To estimate pavement fatigue in 2008, after rehabilitation treatments, unbound layers were calculated using the following equations [10, 11].

$$(3.1) \quad \Delta E_2 = 18.48\epsilon^2 - 55.62\epsilon + 3.80$$

$$(3.2) \quad \Delta E_{sub} = -10.97\epsilon - 1.77$$

$$(3.3) \quad \Delta E_2 = -13.92\epsilon^2 + 36.98\epsilon + 0.58$$

$$(3.4) \quad \Delta E_{sub} = 12.04\epsilon^2 - 20.782\epsilon + 15.17$$

The equations describe the changes in the modulus of the unbound layer due to the unloosing and compacting effects of mining influences. In the first phase of mining deformation, the horizontal unloosing strains are degrading the original modulus [11]. Eq. (3.1) represents the reduction of layer modulus for subgrade, Eq. (3.2) for subbase. The second phase is represented

by consolidation due to road traffic Eq. (3.3), Eq. (3.4). Calculated percentage values of reduction and increase of layer modulus, presented in Table 1, were used to calculate the values of crushed stone aggregate and subgrade modulus presented in Table 2. Table 1 presents calculated percentage changes in subgrade ( $\Delta E_{sub}$ ) and asphalt layer ( $\Delta E_2$ ) moduli due to mining influence. Positive values represent increases, and negative values represent decreases. The analysis divides the mining impact into two phases: an initial phase characterized by horizontal loosening and a later phase dominated by consolidation due to traffic. Across all three sections, the initial phase consistently shows a reduction in the modulus of both the subgrade and asphalt layers, with the greatest reduction observed in Section 1 (8% and 31% respectively). The subsequent phase shows a relative increase in moduli, although these are still substantially lower than initial values. The mining influences from the finished exploitation from the coal of deposit 713 were present from 2008 to 2011 and from deposit 707 from 2016 to 2017 and determined the time periods in Table 2.

Table 1. Calculated percentage values of increase and reduction of layer modulus

Section	$\varepsilon_{average}$ [mm/m]	Increase of modulus		Reduction of modulus	
		$\Delta E_{sub}$ [%]	$\Delta E_2$ [%]	$\Delta E_{sub}$ [%]	$\Delta E_2$ [%]
1	0.6	7	18	8	31
2	0.5	8	15	7	27
3	0.7	7	20	9	33

Table 2 displays the calculated crushed stone aggregate ( $\Delta E_2$ ) and subgrade ( $\Delta E_{sub}$ ) moduli for both reinforced (R) and unreinforced (UN) lanes over the study period (2011, 2016, 2017, 2019). A clear trend indicates a reduction in moduli across all years and sections. This suggests a continuous degradation of the pavement structure due to ongoing traffic loading and potential residual effects of mining subsidence. Notably, there is no consistently observable superior performance in the reinforced lane’s moduli, underscoring the complex interplay between reinforcement effectiveness and mining impact. In some instances (e.g., section 2 in 2019), the reinforced lane demonstrates a significantly lower modulus than the unreinforced lane.

Table 2. Calculated values of crushed stone aggregate modulus  $E_2$  and subgrade modulus  $E_{sub}$

Layer	Section	2011		2016		2017		2019	
		UN	R	UN	R	UN	R	UN	R
Crushed stone aggregate modulus $E_2$ [MPa]	1	294	251	348	297	240	205	283	241
	2	250	170	287	195	210	142	242	164
	3	255	159	305	190	205	127	246	152
Subgrade modulus $E_{sub}$ [MPa]	1	94	58	101	62	94	57	100	61
	2	45	41	48	44	45	40	48	43
	3	63	92	68	100	62	91	66	97

Symbols: UN – unreinforced lane, R – reinforced lane

Initial parameters and a comprehensive summary of initial pavement parameters and calculated fatigue life ( $N_f$ ) for both reinforced (R) and unreinforced (UN) lanes across different years and sections were presented in Table 3.

Table 3. Initial parameters and the results of all analyzed conditions

Section			1	2	3
Asphalt layer modulus, adjusted to the temperature of 20°C $E_{1,tr}$ [MPa]	2008	UN	4360		
		R			
	2019	UN	3312	2078	3228
		R	2910	2710	3006
	2021	UN	2627	1774	2974
		R	3141	1863	2563
Crushed stone aggregate modulus $E_2$ [MPa]	2008	UN	294	250	255
		R	251	170	159
	2019	UN	283	242	246
		R	241	164	152
	2021	UN	214	190	245
		R	183	193	160
Subgrade modulus $E_{sub}$ [MPa]	2008	UN	94	45	63
		R	58	41	92
	2019	UN	100	48	66
		R	61	43	97
	2021	UN	87	68	62
		R	77	77	70
Tensile strain at the bottom of the asphalt layer $\varepsilon_1$ [ $\mu$ strain]	2008	UN	222	180	241
		R	244	206	290
	2019	UN	256	264	281
		R	298	276	363
	2021	UN	321	318	293
		R	329	307	389
The number of load repetitions to failure $N_f$ [mln. ESAL]	2008	UN	0.580	1.156	0.442
		R	0.425	0.741	0.240
	2019	UN	0.459	0.617	0.345
		R	0.311	0.424	0.157
	2021	UN	0.265	0.383	0.322
		R	0.210	0.411	0.144
Traffic load of 100 kN axles $N_{100}$ [mln. ESAL]	2008–2019	UN	0.446		
		R	0.413		
	2019–2021	UN	0.089		
		R	0.078		

Symbols: UN – unreinforced lane, R – reinforced lane

These fatigue life calculations rely on empirical equations, the accuracy of which under Polish conditions, especially considering the complexities of mining subsidence, is not fully established. Consequently, it's not possible to reliably quantify the margin of error associated with these predictions. While this approach is common practice, it's crucial to acknowledge its limitations. The calculations and research indicate that the pavement fatigue of the reinforced lane was greater than that of the unreinforced one. It may suggest that the technical condition of the reinforcement lane was better at the time of rehabilitation treatments. The initial asphalt layer modulus  $E_1$ ,  $t_r$  in 2008 was higher than in the unreinforced lane. Additionally a fatigue calculated by reinforced and unreinforced lanes decreases significantly in the initial period of 2008 to 2019 with a slightly higher decrease in reinforced lanes. This may support the fact that glass fiber mesh was applied to the reinforced lane to address preexisting deficiencies, resulting in worse technical condition in 2008. However, the traffic load was lower in the unreinforced lane. Despite this, it can be observed that unreinforced lane degrades significantly faster after the mining influences stopped (2019–2021), in sections 1 and 2. It can also be observed that the pavement fatigue in sections 1 and 2 decreases much slower between 2019 and 2021 in the reinforced lane. As mentioned above, mining influences were present from 2008 to 2011 and then from 2016 to 2017. This shows the positive influence of applied glass fiber mesh reinforcement on improving pavement fatigue, but only after mining influence retraction. It also suggests that reinforcement in the form of single layer mesh applied at the bottom of asphalt layers improves pavement fatigue in the last phase of the pavement life cycle. Furthermore, the calculated values of pavement fatigue in year 2008 are even 50% lower in the reinforced lane. This also points toward the effectiveness of applying reinforcement to increase pavement fatigue beyond the initial calculated pavement life. The retraction of mining influences is also crucial, because when this phenomena is present, the analyzed reinforcement has no influence on pavement technical condition. This observation emphasizes the importance of considering factors beyond the reinforcement strategy to ensure long-term pavement durability in mining-affected areas. The low calculated  $N_f$  values in 2021, across all sections, also suggest potential inadequacies in the design of the rehabilitation treatments considering the actual traffic loads. Further investigation into the underlying mechanisms, possibly through more detailed analysis of stress distribution within the pavement layers, is necessary.

## References

- [1] J. Kawalec, M. Grygierek, E. Koda, and P. Osiński, "Lessons learned on geosynthetics applications in road structures in Silesia mining region in Poland", *Applied Sciences*, vol. 9, no. 6, art. no. 1122, 2019, doi: [10.3390/app9061122](https://doi.org/10.3390/app9061122).
- [2] P. Zieliński, "Investigations of fatigue of asphalt layers with geosynthetics", *Archives of Civil Engineering*, vol. 59, no. 2, pp. 247–263, 2013, doi: [10.2478/ace-2013-0013](https://doi.org/10.2478/ace-2013-0013).
- [3] W. Janusz, J. Zych, and M. Chudek, *Studium dotyczące stanu rozpoznania tworzenia się i prognozowania deformacji nieciągłych pod wpływem podziemnej eksploatacji złóż*. Gliwice: Politechnika Śląska, 1988.
- [4] M. Zięba, P. Kalisz, and M. Grygierek, "The impact of mining deformations on road pavements reinforced with geosynthetics", *Archives of Mining Sciences*, vol. 65, no. 4, pp. 751–765, 2020, doi: [10.24425/ams.2020.134145](https://doi.org/10.24425/ams.2020.134145).
- [5] Z. Liu and H. Ling, "Performance of geosynthetic-reinforced asphalt pavements", *Journal of Geotechnical and Geoenvironmental Engineering*, vol. 127, no. 2, pp. 177–184, 2001, doi: [10.1061/\(ASCE\)1090-0241\(2001\)127:2\(177\)](https://doi.org/10.1061/(ASCE)1090-0241(2001)127:2(177)).

- [6] P. Jaskuła, D. Ryś, M. Stienss, C. Szydłowski, M. Gołos, and J. Kawalec, "Fatigue performance of double-layered asphalt concrete beams reinforced with new type of geocomposites", *Materials*, vol. 14, no. 9, art. no. 2190, 2021, doi: [10.3390/ma14092190](https://doi.org/10.3390/ma14092190).
- [7] M. Kałuża, "Badania i analizy nawierzchni poddanych oddziaływaniom górniczym", PhD thesis, Silesian University of Technology, Gliwice, 2023.
- [8] M. Kałuża, M. Kotasiński, and J. Bzówka, "Evaluation of the influence of the glass fiber mesh on the deflection basin parameters of a flexible pavement located in the area of mining activity", *Archives of Civil Engineering*, vol. 69, no. 2, pp. 551–569, 2023, doi: [10.24425/ace.2023.145284](https://doi.org/10.24425/ace.2023.145284).
- [9] M. Kałuża and M. Kotasiński, "Relationship between deflection basin parameters and back calculated pavement layer moduli", *Archives of Civil Engineering*, vol. 70, no. 2, pp. 149–162, 2024, doi: [10.24425/ace.2024.149856](https://doi.org/10.24425/ace.2024.149856).
- [10] J. Kawalec, K. Chlipalski, and M. Grygierek, "Komunikacyjne obiekty liniowe na terenach górniczych", *Magazyn Autostrady*, vol. 2015, no. 3, pp. 35–42, 2015.
- [11] M. Grygierek and A. Waszak, "Zmiana sztywności nawierzchni drogowej w obszarze deformacji nieciągłej", *Przegląd Górniczy*, vol. 71, no. 3, pp. 30–37, 2015.

## Wpływ siatki z włókna szklanego na trwałość zmęczeniową nawierzchni podatnej wstępnie zdegradowanej

**Słowa kluczowe:** metoda mechanistyczno-empiryczna, nawierzchnie podatne, oddziaływania górnicze, siatka z włókna szklanego, trwałość nawierzchni, ugięciomierz FWD

### Streszczenie:

W trakcie prowadzonych prac remontowych wykonano wzmocnienie jednego z pasów ruchu jezdni siatką z włókna szklanego. Geosyntetyk zabudowano w spodzie warstw z betonu asfaltowego, natomiast drugi pas ruchu wykonano bez zastosowania wzmocnienia. Aby ocenić stan techniczny nawierzchni drogi, wykorzystano pomiary ugięciomierzem FWD w celu wyznaczenia modułów sprężystości warstw, co było niezbędne do zbadania nośności konstrukcji jezdni. Trwałość zmęczeniowa nawierzchni została obliczona oraz porównana z pomierzonym i przewidywanym obciążeniem ruchem drogowym. Wyniki wskazują, że zastosowanie wzmocnienia siatką z włókna szklanego pozytywnie wpłynęło na nośność i trwałość nawierzchni. Korzystne efekty były obserwowane dopiero po zakończeniu działalności górniczej, której oddziaływania spowodowały pierwotne uszkodzenia nawierzchni. Trwałość zmęczeniowa, określona dla obciążenia dynamicznego oraz przewidywanego obciążenia ruchem, została porównana pomiędzy pasem jezdni wzmocnionym a niewzmocnionym. Stwierdzono, że pas wzmocniony wykazał lepszą odporność na postępującą degradację nawierzchni po ustaniu oddziaływań górniczych.

Received: 2024-11-20, Revised: 2025-03-02